

## Mesoscopic Donor–Acceptor Multilayer by Ultrahigh-Vacuum Codeposition of Zn-Tetraphenyl-Porphyrin and C<sub>70</sub>

Paolo Vilmercati,<sup>†,‡</sup> Carla Castellarin-Cudia,<sup>†</sup> Ralph Gebauer,<sup>§,||</sup> Prasenjit Ghosh,<sup>§</sup>  
Silvano Lizzit,<sup>†</sup> Luca Petaccia,<sup>†</sup> Cinzia Cepek,<sup>⊥</sup> Rosanna Larciprete,<sup>#</sup>  
Alberto Verdini,<sup>⊥</sup> Luca Floreano,<sup>⊥</sup> Alberto Morgante,<sup>‡,⊥</sup> and Andrea Goldoni<sup>\*†</sup>

*Sincrotrone Trieste S.C.p.A., s.s. 14 km 163.5 in Area Science Park, 34012 Trieste, Italy,  
Dipartimento di Fisica, Università di Trieste, Via Valerio 2, 34100 - Trieste, Italy, International  
Center for Theoretical Physics (ICTP), Strada Costiera 11, 34014 Trieste, Italy, National Simulation  
Center INFN-Democritos, s.s. 14 km 163.5 in Area Science Park, 34012 Trieste, Italy, National  
Laboratory TASC-INFN-CNR, s.s. 14 km 163.5 in Area Science Park, 34012 Trieste, Italy, and CNR,  
Institute of Complex Systems, Via Fosso del Cavaliere 100, 00133 Roma, Italy,*

Received September 9, 2008; E-mail: andrea.goldoni@elettra.trieste.it

**Abstract:** The peculiar electrochemical and photophysical properties of porphyrin and fullerene molecules make them promising candidates for the construction of two- and three-dimensional organic-based materials. An important question is how pristine fullerene and porphyrin will organize when deposited on surfaces via in vacuum molecular beam evaporation. Here we show that codeposition of C<sub>70</sub> and Zn-tetraphenyl-porphyrin (ZnTPP) induces the self-assembly of electron-rich flat aromatic molecules at the curved surface of C<sub>70</sub>, thus enhancing the chromophore interaction and forming a supramolecular multilayer donor–acceptor structure. While the ground-state electronic spectra almost reflect a simple summation of ZnTPP and C<sub>70</sub> components, the excited-state electrons at the porphyrin macrocycle can rapidly delocalize to the fullerene. The excited charge transfer time scale is faster than 1–2 fs, as shown by resonant photoemission for the core-excited charges.

### Introduction

Molecular and supramolecular donor–acceptor dyads capable of undergoing light-induced energy and electron transfer have been widely studied as photochemical molecular devices that mimic natural photosynthesis reactions.<sup>1–7</sup> In particular, donor–acceptor systems can be used in dye-sensitized semiconductor solar cells and organic dye solar cells.<sup>3</sup> Important parameters in describing the organic solar cells are the photon production of exciton, the separation of the exciton at the donor–acceptor interface, and the transport properties of the separated charge.<sup>3,8</sup>

The composition, interchromophore distance, and orientation, as well as the electronic levels coupling, are important factors in modulating the electron-transfer efficiency, the lifetime of the charge-separated state, and the transport properties.<sup>1–10</sup> To achieve efficient intramolecular electron-transfer processes, both covalent chemistry and biomimetic self-assembly methodologies, such as the formation of  $\pi$  stacks, hydrogen bonds, and van der Waals contacts, have been successfully utilized to connect the donor–acceptor systems. In the majority of these studies, porphyrins or phthalocyanines have been used as photosensitizers and a variety of electron acceptors have been employed.<sup>1–10</sup>

Among the different electron acceptors employed, fullerenes have become the ultimate electron acceptor owing to favorable reduction potentials and small reorganization energies in electron-transfer reactions. As a consequence, fullerenes promote photoinduced charge separation but retards the charge-recombination process, which results in the formation of much desired long-lived charge-separated states.<sup>8–10</sup>

To gain more insight into the influence of molecular topology on electron transfer, a few porphyrin–fullerene dyads in which

<sup>†</sup> Sincrotrone Trieste S.C.p.A.

<sup>‡</sup> Università di Trieste.

<sup>§</sup> International Center for Theoretical Physics (ICTP).

<sup>||</sup> National Simulation Center INFN-Democritos.

<sup>⊥</sup> National Laboratory TASC-INFN-CNR.

<sup>#</sup> CNR, Institute of Complex Systems.

- (1) Guldi, D. M.; Luo, C.; Prato, M.; Troisi, A.; Zerbetto, F.; Scheloske, M.; Dietel, E.; Bauer, W.; Hirsch, A. *J. Am. Chem. Soc.* **2001**, *123*, 9166.
- (2) Sun, D.; Tham, F. S.; Reed, C. A.; Boyd, P. D. W. *Proc. Natl. Acad. Sci. U.S.A.* **2002**, *99*, 5088.
- (3) Ruani, G.; Fontanini, C.; Murgia, M.; Taliani, C. *J. Chem. Phys.* **2002**, *116*, 1713. (a) Heutz, S.; Sullivan, P.; Sanderson, B. M.; Schultes, S. M.; Jones, T. S. *Solar Energy Mat. Solar Cell* **2004**, *83*, 229.
- (4) Milanesio, M. E.; Gervaldio, M.; Otero, L. A.; Sereno, L.; Silber, J. J.; Durantini, E. N. *J. Phys. Org. Chem.* **2002**, *15*, 844.
- (5) Mizuseki, H.; Igarashi, N.; Majumder, C.; Belosludov, R. V.; Farajian, A. A.; Wang, J.-T.; Chen, H.; Kawazoe, Y. *Mater. Res. Soc. Symp. Proc.* **2002**, *725*, 14.1.
- (6) Brousse, B.; Ratier, B.; Moliton, A. *Thin Solid Films* **2004**, *451–452*, 81.
- (7) Boyd, P. D. W.; Reed, C. A. *Acc. Chem. Res.* **2005**, *38*, 235.

- (8) Sakata, Y.; Imahori, H. *Adv. Mater.* **1997**, *9*, 537. (a) Peumans, P.; Uchida, S.; Forrest, S. *Nature* **2003**, *425*, 158. (b) Kobori, Y.; Yamauchi, S.; Akiyama, K.; Tero-Kubota, S.; Imahori, H.; Fukuzumi, S.; Norris, J. R., Jr. *Proc. Natl. Acad. Sci. U.S.A.* **2005**, *102*, 10017.
- (9) Armadori, N.; Marconi, G.; Echegoyen, L.; Bourgeois, J. P.; Diederich, F. *Chem.—Eur. J.* **2000**, *6*, 1629.
- (10) D'Souza, F.; Maligaspe, E.; Karr, P. A.; Schumacher, A. L.; El Ojaimi, M.; Gros, C. P.; Barbe, J.-M.; Ohkubo, K.; Fukuzumi, S. *Chem.—Eur. J.* **2008**, *14*, 674.

the  $\pi$  systems are structurally forced into a face-to-face arrangement have been elegantly designed and studied.<sup>1,2,7</sup> The majority of these studies used some molecular linker to connect the fullerene to the porphyrin, while only few were related to a direct face-to-face bonding between the curved chromophore of fullerene and flat chromophore of porphyrin (typically in solutions or in cocrystals). Controlling the nature of supramolecular self-assembly by noncovalent interactions is a challenge in science and technology that, when overcome, can lead to a breakthrough in the creation of new molecular devices.

In the present study we report a nanostructured multilayer of porphyrin/fullerene pairs obtained by codeposition of Zn-tetraphenyl-porphyrin (ZnTPP) and  $C_{70}$  in ultrahigh-vacuum by powder sublimation. The interaction between the two molecular species was studied *via* high-resolution X-ray photoemission (XPS), UV-ray photoemission (UPS), and Near Edge X-ray Absorption Fine Structure (NEXAFS). The occurrence of an average preferential orientation was determined by angular dependent NEXAFS using linearly polarized monochromatic synchrotron radiation. These measurements were complemented by density-functional based computations for an isolated pair of ZnTPP+ $C_{70}$ , allowing us to study the involved electronic states and the intermolecular charge transfer.

The time scale of excited charge delocalization was then studied by resonant photoemission (ResPES). This technique is equivalent to a pump-and-probe experiment, where one electron is *pumped* from a core level to an empty bond state, and the decay channels of the core hole are studied. The balance between the resonant and the nonresonant decay channel is a fingerprint of the fast delocalization of the excited charge.<sup>11</sup> Because the photon energy is across a core ionization threshold, this technique provides the chemical specificity of core level spectroscopy and the core-hole lifetime gives an upper limit for the time scale of the excited electron delocalization.

Our studies indicate the existence of charge-transfer interactions between the electron-rich ZnTPP and the electron-deficient fullerene. The resulting face-to-face geometry of the dyads, which is in agreement with calculations, allows efficient photoinduced electron transfer from the excited state of the ZnTPP moiety to the  $C_{70}$  moiety to produce the charge-separated state at a time faster than 1–2 fs.

## Experimental Section

All data were collected at the Elettra synchrotron radiation source. The XPS, UPS, ResPES, and NEXAFS measurements were performed at the SuperESCA beamline. Photoelectrons were collected by a double-pass hemispherical analyzer, with an energy resolution better than 100 meV. The NEXAFS measurements were performed in Auger yield mode, i.e., collecting the electron in the kinetic energy range of  $260 \pm 0.5$  eV for the C1s edge and  $370 \pm 0.5$  eV for the N1s edge. The angular dependent NEXAFS experiment was carried out at the ALOISA beamline, and the measurements were performed in partial electron yield mode.<sup>12</sup> The total resolution for NEXAFS at SuperESCA is better than 70 meV and at ALOISA is better than 100 meV.

The codeposited multilayers were grown over a Si(111) surface. The surface was cleaned in an ultrahigh vacuum, base pressure  $10^{-10}$  mbar, by annealing at 900 °C. The absence of contaminants was checked by XPS, and the  $(7 \times 7)$ -reconstructed surface was

observed by low energy electron diffraction (SuperESCA) and reflected high-energy electron diffraction (ALOISA).

We choose  $C_{70}$  (instead of the commonly used  $C_{60}$ ) because the orientation of the molecule can be determined by NEXAFS thanks to its axial anisotropy.

The molecular films were obtained by powder sublimation (molecules produced by Sigma Aldrich) using two Kundsens cells. The base pressure in the preparation never exceeded  $8 \times 10^{-10}$  mbar during the evaporation. The temperature of the two Kundsens cells was set to obtain the same evaporation rate for each molecular species. The evaporation rate of each cell was estimated by core level XPS spectra as a function of molecular coverage. The thickness of the codeposited films was in the range  $110 \pm 40$  nm.

## Results and Discussion

**XPS.** As shown by Castellarin-Cudia and co-workers,<sup>13</sup> for a ZnTPP molecule in a multilayer film the four nitrogen atoms of the macrocycle are chemically equivalent, like in an isolated ZnTPP molecule. Therefore, the measured XPS spectra are simply composed by a single peak.

Recently we realized a porphyrin/fullerene junction depositing a single porphyrin layer on top a single  $C_{70}$  layer first deposited on the freshly cleaned Si(111)- $(7 \times 7)$  reconstructed surface.<sup>14</sup> In the following we will refer to this system as the *double layer*. When  $C_{70}$  and porphyrin are assembled in a *double layer* structure, where the fullerenes are forced to stand up with respect to the surface and consequently the porphyrin is forced to lie atop the fullerene (which is a quite different geometry with respect to the calculated “side-on” bonding configuration), a splitting of the N1s peak was detected.<sup>14</sup> In that particular case the four nitrogen atoms of the macrocycle point to the center of two hexagons and of two pentagons near the top of the  $C_{70}$  molecule, and consequently, the energy configuration is different from that described by theory where structures are optimized and the free energy is minimum.

On the contrary, as can be seen in Figure 1, in the codeposited system the N1s spectrum is similar to that of the ZnTPP multilayer; it presents the same full width at half-maximum, and the nitrogen atoms are, therefore, chemically equivalent. The only difference is a very small binding energy shift of 100 meV of the N1s spectrum when compared with the pristine ZnTPP multilayer, indicating that in the codeposited system the molecules are free to assemble and the geometrical configuration they assume is due to the minimization of the interaction energy with a very small amount of charge reorganization.

Similar information is obtained by the C1s core level photoemission spectra reported in Figure 2. The binding energy of the codeposited spectrum is in between the two pristine systems ( $C_{70}$  at lower binding energy and ZnTPP at higher binding energy).

The line shape of the codeposited spectrum is a combination of the two pristine spectra. Just by a summation of the two pristine spectra, with the ratio ZnTPP/ $C_{70} \approx 2.5$  with respect to the stoichiometric ratio considering one  $C_{70}$  and one porphyrin (there is a redundancy of ZnTPP, which means that the surface is probably terminated by ZnTPP), we can reproduce quite well the codeposited spectrum.

(11) Brühwiler, P. A.; Karis, O.; Mårtensson, N. *Rev. Mod. Phys.* **2002**, *74*, 703.

(12) Floreano, L.; Cossaro, A.; Gotter, R.; Verdini, A.; Bavdek, G.; Evangelista, F.; Ruocco, A.; Morgante, A.; Cvetko, D. *J. Phys. Chem. C* **2008**, *112*, 10794.

(13) Castellarin Cudia, C.; Vilmercati, P.; Larciprete, R.; Cepek, C.; Zampieri, G.; Sangaletti, L.; Pagliara, S.; Verdini, A.; Cossaro, A.; Floreano, L.; Morgante, A.; Petaccia, L.; Lizzit, S.; Battocchio, C.; Polzonetti, G.; Goldoni, A. *Surf. Sci.* **2006**, *600*, 4013.

(14) Vilmercati, P.; Castellarin Cudia, C.; Larciprete, R.; Cepek, C.; Zampieri, G.; Sangaletti, L.; Pagliara, S.; Verdini, A.; Cossaro, A.; Floreano, L.; Morgante, A.; Petaccia, L.; Lizzit, S.; Battocchio, C.; Polzonetti, G.; Goldoni, A. *Surf. Sci.* **2006**, *600*, 4018.

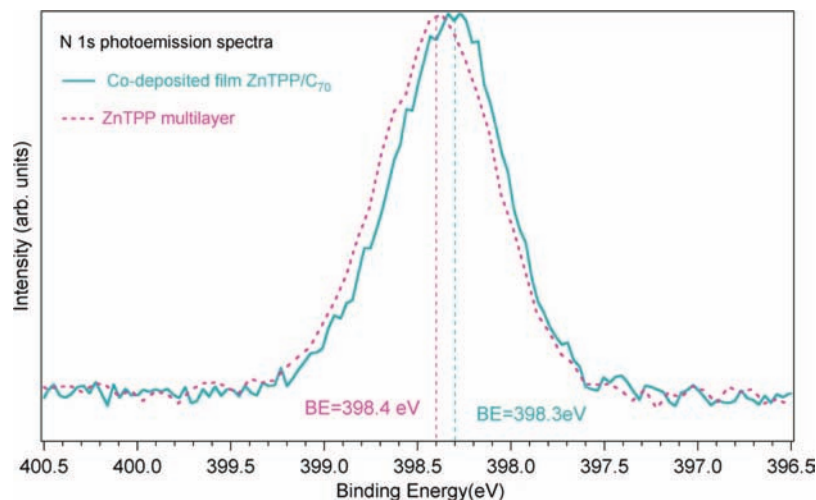


**Figure 1.** N1s spectra of the pristine ZnTPP multilayer and of the codeposited C<sub>70</sub>+ZnTPP multilayer. The spectra were measured at  $h\nu = 550$  eV.

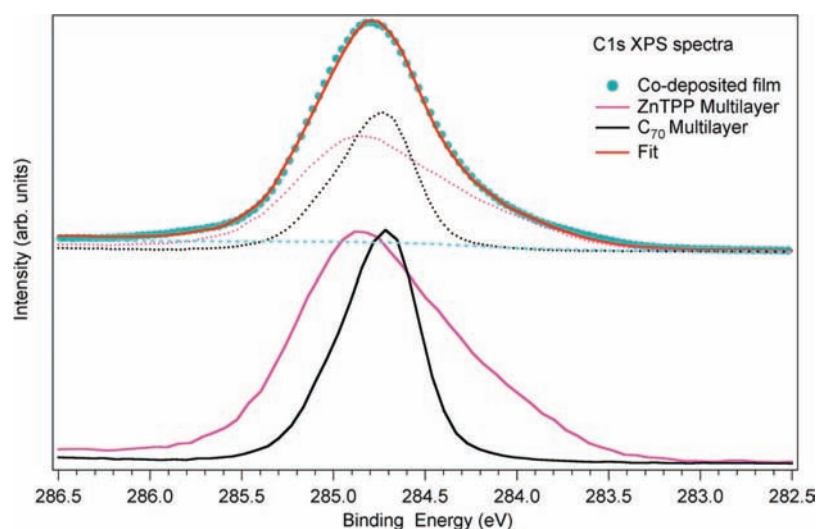


**Figure 2.** C1s spectra of the pristine C<sub>70</sub>, the pristine ZnTPP multilayer and the codeposited C<sub>70</sub>+ZnTPP multilayer. The fit using the pristine components (dashed lines), with the relative weight, is also shown. The spectra were measured at  $h\nu = 400$  eV.

N1s and C1s XPS spectra are both the fingerprint of the electrostatic interaction and of the charge displacement between the ZnTPP and the C<sub>70</sub> which, apparently (simply judging from the relative shifts with respect to the pristine molecules), is from porphyrin to C<sub>70</sub>.

**NEXAFS.** Figure 3 shows the NEXAFS at the N1s edge of the codeposited system. The first peak in the NEXAFS spectrum corresponds to the transition from the N1s core level to the LUMO+4 ( $\pi_1^*$ ) of the complex, while the successive two peaks are due to transitions to higher  $\pi^*$  energy levels and above 409–410 eV to  $\sigma^*$  states (see the supporting material).

The dichroism of the N1s spectrum as a function of the angle between the linear polarization of the light and the surface would describe how the porphyrin macrocycle is oriented.<sup>15</sup> The NEXAFS spectra of the codeposited system show a clear dependence of the  $\pi^*$  states of the macrocycles from the polarization vector of the impinging radiation, indicating that there is a preferential molecular orientation. To obtain this

molecular orientation we have plotted in the inset of Figure 3 the intensity ratio between the first  $\pi_1^*$  state as a function of the angle  $\theta$  between the polarization vector and the normal to the surface plane. Because the substrate is Si(111), the best fit is obtained using a function that describes three or more domains of orientation in the plane:<sup>15</sup>

$$I_{\pi_1^*} = 1 - \cos^2 \theta \cos^2 \gamma - \frac{1}{2} \sin^2 \theta \sin^2 \gamma$$

The only fitting parameter is the angle  $\gamma$  that the macrocycle plane forms with the surface. The result is  $\gamma = 47.8 \pm 2.5^\circ$  and obviously is independent from the azimuth. However, as noted by Glowatzki et al.<sup>16</sup> in a recent paper, apart from the cases where the macrocycle is flat or perpendicular to the substrate, in the intermediate cases the angle obtained by NEXAFS might be equally due to the superposition of two or more orientations. Since we have no complementary diffraction

(15) Stöhr J. *NEXAFS Spectroscopy*; Springer Series in Surface Science 25; Springer: Berlin, 1992..

(16) Glowatzki, H.; Gavrilu, G. N.; Seifert, S.; Johnson, R. L.; Räder, J.; Müllen, K.; Zahn, D. R. T.; Rabe, J. P.; Koch, N. *J. Phys. Chem. C* **2008**, *112*, 1570.

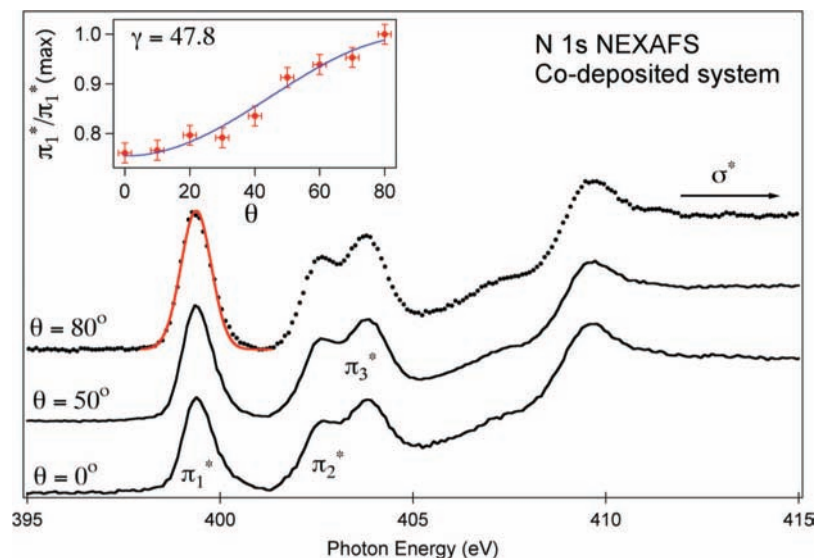


**Figure 3.** NEXAFS spectra at the N1s threshold as a function of the angle  $\theta$  between the substrate normal and the polarization vector of the light for some chosen angle. The Gaussian fit of the  $\pi_1^*$  peak in the  $\theta = 80^\circ$  spectrum is also shown. The inset reports the ratio  $\pi_1^*/\pi_1^*(\max)$  as a function of  $\theta$  and the relative fit.<sup>15</sup>

data to compare with the NEXAFS, we rather refer to the molecular orientation  $\gamma$  as the “average angle” of the macrocycle.

From the NEXAFS spectra at the C1s edge we can obtain further information about the geometrical configuration of the system. Figure 4a shows the C1s NEXAFS measured at SuperESCA (normal incidence of the light,  $70^\circ$  of emission) on the pristine ZnTPP and C<sub>70</sub> multilayers, the linear combination of these two spectra, and the spectrum of the codeposited film.

The absorption spectrum at the C1s threshold of the codeposited film contains clearly the features of the two component molecules. Similarly to the photoemission core level spectra, the NEXAFS can be almost completely composed by a summation of the C<sub>70</sub> and porphyrin spectra with the ratio ZnTPP/C<sub>70</sub>  $\approx 1.5$  with respect to the stoichiometric ratio (as defined for the XPS spectra).

Figure 4b shows the C1s NEXAFS spectra measured at the ALOISA beamline on the codeposited film as a function of the angle between the surface and the linear electrical field of the synchrotron radiation. Because of the peculiar grazing incidence geometry at this beamline,<sup>12</sup> which is kept at  $6^\circ$ , and due to the fact that the spectra were taken in partial yield mode, these spectra appeared a bit different from the one presented in Figure 4a. In particular the macrocycle porphyrin peak at 284.2 eV is more evident. Also in this way, looking at the dichroism that some peaks display as a function of the light polarization, we can detect the porphyrin and, possibly, the C<sub>70</sub> orientations.

As before, the angular dependence of the first excitation belonging to the porphyrin reflects the behavior of the  $\pi^*$  states located at the macrocycle. As for the N1s NEXAFS spectra, the best fit was obtained using the same model function for more than three azimuthal orientations. The angle  $\gamma = 46.8 \pm 2.5^\circ$  obtained for this state confirms the evaluation at the N1s edge for the average angle that the macrocycle plane forms with the surface. It is a good confirmation that in the C1s NEXAFS spectrum of the complex system the first excitation belongs only to the porphyrin and a very small superposition with other states occurs.

Let us consider now the carbon atoms of C<sub>70</sub>. They form closed chains of atoms at the C<sub>70</sub> cage, starting with the

pentagons at the top and at the bottom of the molecule (C1 atoms<sup>17,18</sup>) and ending with the C5 chain atoms at the shortest equator.<sup>17,18</sup> The dichroism of the corresponding peaks would describe, although not in an easy manner, the orientation of the long axis of the molecule<sup>18</sup> and, therefore, how the molecule is oriented. However, looking at the first peak at  $\sim 284.5$  eV, which belongs almost completely to C<sub>70</sub>, it seems that there is no variation of the intensity. This can be simply interpreted as the C<sub>70</sub> is disordered, but the disorder must be a rotation in a plane almost parallel to the porphyrin macrocycle. In fact if there were C<sub>70</sub> positions with the long axis perpendicular to the macrocycles, this should also reflect in the XPS spectra. In particular the N1s spectra should be much broader than what is observed in this system (see for example the N1s spectrum of the *double-layer*<sup>14</sup>). Another possibility, however, is that C<sub>70</sub> has the long axis at the magic angle, i.e., at  $\sim 35.3^\circ$  with respect to the substrate surface; therefore it would be almost parallel to the macrocycle plane with a tilted angle of  $\sim 12 \pm 5^\circ$ .

In both cases, C<sub>70</sub> accommodates in a “side-on” rather than “end-on” orientation, with its 5-fold axis possibly a bit tilted with respect to the porphyrin macrocycle plane. This is the expected result of maximizing the van der Waals contact, which, from molecular mechanics modeling,<sup>19</sup> is the fundamental basis of the fullerene–porphyrin interaction. A similar orientation is observed in the discrete supramolecular chemistry of jaws porphyrin<sup>20</sup> and cocrystallite structures.<sup>4,21–24</sup> For example in CuTPP+C<sub>70</sub> cocrystals<sup>21</sup> the macrocycle is nearly parallel ( $10^\circ$ ) to the long axis of the ellipsoidal C<sub>70</sub>. The same “side-on” approach of C<sub>70</sub> to porphyrin was found in cocrystal of ZnTPP+C<sub>70</sub><sup>24</sup> and in the series of isostructural complexes.<sup>23</sup> In this case the long axis of the C<sub>70</sub> is inclined by  $\sim 16^\circ$  with respect to the porphyrin plane. This arrangement contrasts with the “end-

(17) Nyberg, M.; Luo, Y.; Triguero, L.; Pettersson, L. G. M.; Ågren, H. *Phys. Rev. B* **1999**, *60*, 7956.

(18) Goldoni, A.; Cepek, C.; Larciprete, R.; Sangaletti, L.; Pagliara, S.; Floreano, L.; Gotter, R.; Verdini, A.; Morgante, A.; Luo, Y.; Nyberg, M. *J. Chem. Phys.* **2002**, *116*, 7685.

(19) Lin, Z.; Wang, Y.-B. *J. Am. Chem. Soc.* **2003**, *125*, 6072.

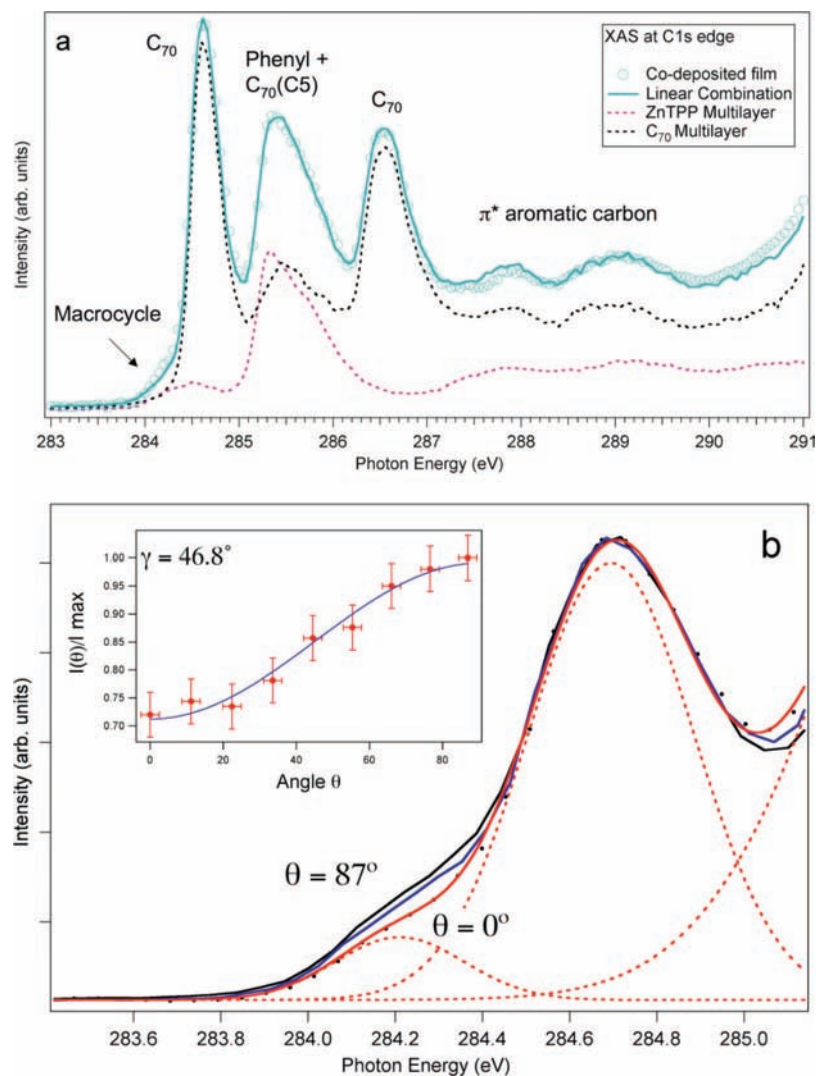


**Figure 4.** NEXAFS at the C1s threshold of the codeposited film. (a) The codeposited spectrum can be reproduced by a linear combination of the C<sub>70</sub> and ZnTPP pristine spectra (see text). (b) Dependence of the spectral features (macrocycle and first C<sub>70</sub> peaks) as a function of the angle  $\theta$  between the substrate normal and the polarization vector of the light. The fit of the spectrum at  $\theta = 0^\circ$  is shown with the components (dashed lines). The inset shows the intensity of the first  $\pi^*$  transition as a function of  $\theta$  and the relative fit.<sup>15</sup>

on" coordination of C<sub>70</sub> with metal surfaces, which occurs when the back-bonding interaction is significant.<sup>18,25</sup>

**ResPES at C1s Ionization Edge.** In Figure 5 the photoelectron intensity in the valence band is shown as the photon energy scans through the absorption edge of the C1s core level. At the top is a plot of the valence band measured before the ionization edge, at 278.8 eV. At the left side the NEXAFS spectrum measured in Auger yield mode is plotted. In the picture the sharp enhancement in the low binding energy region between 0 and 9 eV, in correspondence of the excitation in the NEXAFS

spectrum between 285 and 287 eV, is clearly visible. These are the resonant contributions to the spectrum belonging to participator and spectator decays. Since our spectra are plotted in the binding energy region, the strong carbon KVV Auger emission is visible as a linear dispersion in binding energy (constant in kinetic energy) in the higher energy part of the spectrum. Instead, in the low binding energy region a small dispersing intensity due to the C1s core level excited by the second diffraction order of the monochromator is visible. For example, for the first spectrum taken at  $h\nu = 278.8$  eV, this peak is at 6.5 eV, and it is distinguishable because it follows the dispersion in kinetic energy of two times the photon energy. For an appropriate data analysis of the resonant photoemission spectra, the Auger and the second diffraction order peaks must be removed (see Supporting Information). Finally, the strong intensity at 10.3 eV is due to the Zn3d core levels that lie in the valence band region.

The bottom panel of Figure 6 shows a collection of the valence band spectra obtained at the photon energies corresponding to the maxima in the absorption spectrum, after the Shirley background (proportional to the full spectrum) and the Auger subtraction. The second spectrum is taken at  $h\nu = 284.2$

- (20) Sun, D.; Tham, F. S.; Reed, C. A.; Chaker, L.; Burgess, M.; Boyd, P. D. W. *J. Am. Chem. Soc.* **2000**, *122*, 10704.
- (21) Konarev, D. V.; Neretin, I. S.; Slovokhotov, Y. L.; Yudanova, E. I.; Drichko, N. V.; Shul'ga, Y. M.; Tarasov, B. P.; Gumanov, L. L.; Batsanov, A. S.; Howard, J. A. K.; Lyubovskaya, R. N. *Chem.—Eur. J.* **2001**, *7*, 2605.
- (22) Ishii, T.; Aizawa, N.; Kanehama, R.; Yamashita, M.; Sugiura, K.; Miyasaka, H. *Coord. Chem. Rev.* **2002**, *226*, 113.
- (23) Olmstead, M. M.; Costa, D. A.; Maitra, K.; Noll, B. C.; Phillips, S. L.; Van Calcar, P. M.; Balch, A. L. *J. Am. Chem. Soc.* **1999**, *121*, 7090.
- (24) Boyd, P. D. W.; Hodgson, M. C.; Rickard, C. E. F.; Oliver, A. G.; Chaker, L.; Brothers, P. J.; Bolskar, R. D.; Tham, F. S.; Reed, C. A. *J. Am. Chem. Soc.* **1999**, *121*, 10487.
- (25) Balch, A. L.; Olmstead, M. M. *Chem. Rev.* **1998**, *98*, 2123.

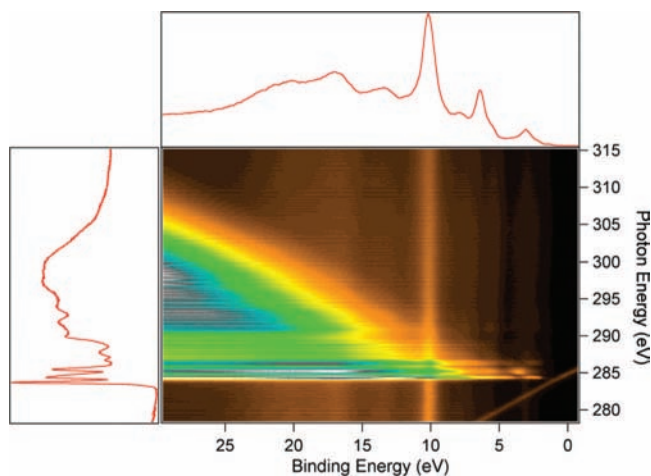


**Figure 5.** Full resonant spectrum of the codeposited system scanning the C1s threshold. On the left side there is the NEXAFS spectrum at the C1s edge along which the resonance has been taken and on the top part the valence band measured before the resonance at photon energy of 278.8 eV. The main dispersing features are the KVV Auger peaks, whereas the weak dispersing feature at the low binding energy is the C1s peak excited by the second order radiation.

eV of excitation energy, i.e., the energy of the porphyrin macrocycle structure in the NEXAFS spectrum. This spectrum closely resembles the nonresonant spectrum ( $h\nu = 278.8$  eV), and no clear resonant decay is detected. This means that when the electron is excited from an atom belonging to the macrocycle, the excitation is transferred away from the excited atom on a time scale faster than the core-hole lifetime. This charge transfer could occur from the porphyrin to the porphyrin itself (just to neighbor atoms or molecule) or to the  $C_{70}$ .

At an energy of 284.6 eV, i.e., when the excitation is localized at the first intense peak, an evident electron enhancement is detected. Since this excitation peak mainly belongs to  $C_{70}$  this allows the assignments of the enhanced state in valence band to the  $C_{70}$  and shows that an electron excited to the  $C_{70}$  cage remains localized for a time longer than the core hole lifetime. This is more evident after subtracting the nonresonant spectrum at 278.8 eV and integrating all the resonant contributions between 0 and 9 eV (leaving out the Zn3d peak) to obtain the “pure resonant” spectrum, which can be compared with the NEXAFS spectrum.

When normalized to the same intensity at 285.4 eV, there are some important differences between the two spectra (Figure 6, top panel). The resonant photoemission intensity is, for some photon energy, quite screened or completely absent indicating that for these photon energies the excited electron is suddenly transferred to another molecule or to another atom. If we compare the pure resonant spectrum with the pristine porphyrin multilayer resonant spectrum,<sup>13</sup> we could note that in the latter case a clear resonant contribution is detectable in correspondence to the excitation into the  $\pi^*$  states of the macrocycle, demonstrating a competition between the decay channels and the ultrafast charge delocalization of the excited charge. In our case, instead, the resonance is completely quenched when we excite electrons in the macrocycle; therefore the ultrafast delocalization should occur between the porphyrin and the  $C_{70}$ , indicating that, at this energy, the porphyrin acts as the electron donor and the  $C_{70}$  as the electron acceptor.

This is also true, but in the opposite way, for the third absorption peak at 286.6 eV that belongs to  $C_{70}$ , which is strongly attenuated with respect to the NEXAFS spectrum.

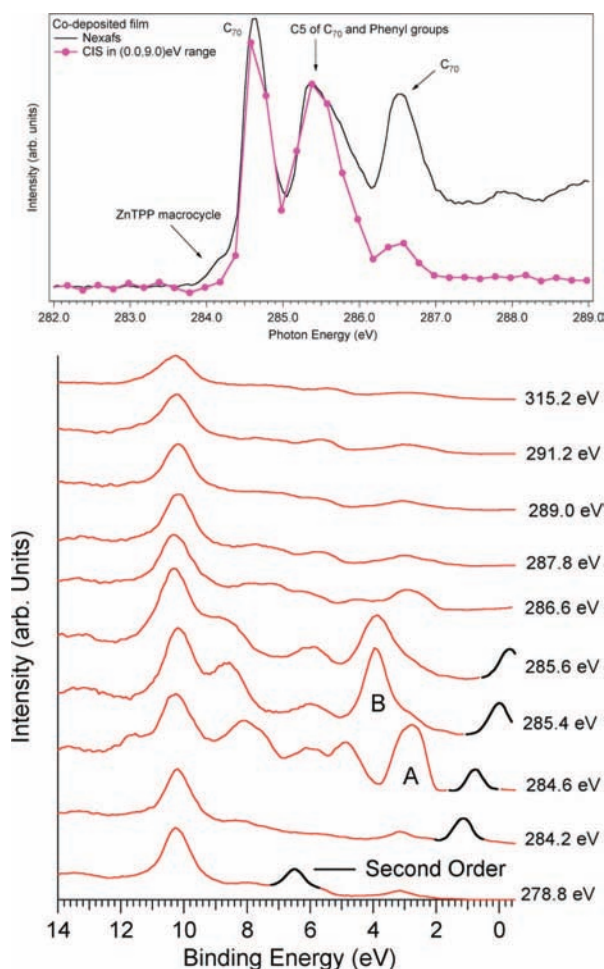


**Figure 6.** (Top panel) NEXAFS spectrum at the C1s threshold compared to the “pure resonant” spectrum (see text) obtained by integrating in the range 0–9 eV of binding energy the valence band at each photon energy. (Bottom panel) A selection of resonant photoemission spectra at different photon energies across the C1s threshold after the Auger and background subtraction, corresponding to the maxima in the C1s NEXAFS spectrum shown above. The peak due to second-order radiation that overlaps the valence band has been shown as a black line.

The time scale of these charge transfers can be obtained by looking at the Fano profile of some resonant features.<sup>26,27</sup> In Figure 7 we plot the resonant behavior or constant initial state profile (CIS) of the resonant features A and B in Figure 6 and the corresponding fit with the Fano profile  $I = (q + \epsilon)^2 / (1 + \epsilon^2)$  where  $q$  is the asymmetry parameter,  $\epsilon = (E - E_{\text{res}}) / \Gamma$ , and  $E_{\text{res}}$  and  $\Gamma$  are the energy and the spectral half-width of the resonance, respectively.<sup>27</sup> The spectral width of the resonance is given by  $2\Gamma = \sum_{ij} V_{ij}$ , i.e., the superposition of all the matrix elements of the processes  $ij$  involved in the de-excitation of the core hole.<sup>27</sup> Therefore  $2\Gamma$  is a measure of the lifetime of the core hole ( $\tau = \hbar / 2\Gamma$  or  $\tau = \hbar / 4\pi\Gamma$ ). Although these profiles correspond to different parameters due to the fact that the core hole is excited from different carbon atoms, it is evident that the charge transfer time scale should be much shorter than 1–2 fs to not observe the resonant behavior.

(26) Weinelt, M.; Nilsson, A.; Magnuson, M.; Wiell, T.; Wassdahl, N.; Karis, O.; Föhlisch, A.; Stöhr, N. M. J.; Samant, M. *Phys. Rev. Lett.* **1997**, *78*, 967.

(27) Fano, U. *Phys. Rev.* **1961**, *124*, 1866.

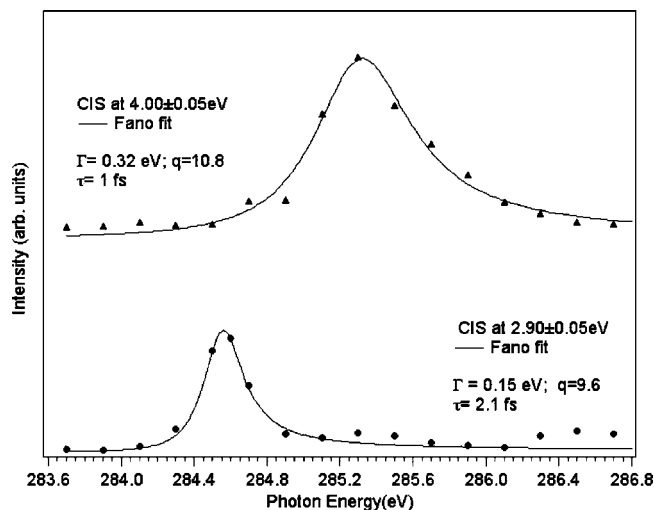


**Figure 7.** CIS spectra of the resonant features A (bottom) and B (top) of Figure 6 and the corresponding fit with a Fano profile. The fit parameters and the resulting hole-lifetime  $\tau$  are also reported.

## Computational Results

Previous calculations<sup>19</sup> for a system of ZnTPP+C<sub>70</sub> predicted a prevalently electrostatic binding interaction. By describing the potential surfaces of pristine ZnTPP, pristine C<sub>70</sub>, and complex ZnTPP+C<sub>70</sub>, those calculations indicate that the interaction responsible for the bonding between the two molecules involves the nitrogen atoms of the porphyrin and the center of three hexagons and one pentagon in C<sub>70</sub>. The C<sub>70</sub> stays in a “side-on” bonding configuration with the long axis almost parallel to the porphyrin macrocycle. In particular, the calculated equilibrium configuration predicts the porphyrin at a distance of 2.9 Å from the fullerene and a charge transfer from the porphyrin to the fullerene of ~0.13 electrons/molecule.

We have also performed density-functional calculations of the structural and electronic properties of the metalloporphyrin+C<sub>70</sub> system. Using the quantum-ESPRESSO code,<sup>28</sup> a plane-wave basis set was used with a kinetic energy cutoff of 25 and 210 Ry for the electronic orbitals and the charge density, respectively. The molecules were placed in an orthorhombic box of 25 Å × 25 Å × 27.3 Å sides to which periodic boundary conditions were applied. The PBE<sup>29</sup> functional was used for exchange-correlation energies, and the electron–ion interaction was described using ultrasoft pseudopotentials.<sup>30</sup> Structural relaxations of the metalloporphyrin–C<sub>70</sub> system were performed to determine the lowest energy geometry. In those relaxations, the distance between the Zn atom and the center of the closest 6:6 bond of the fullerene was constrained to the experimental value 2.8 Å.<sup>30</sup> This procedure was chosen to account for the well-known incapacity of the density functional to correctly describe bond lengths in such weakly bound systems.

Our calculations find a “side-on” orientation of the C<sub>70</sub> molecule with respect to the macrocycle of the porphyrin, similar to what was obtained by Wang et al.<sup>19</sup> with a C<sub>70</sub>–porphyrin distance of 2.9 Å. The angle between the long axis of C<sub>70</sub> and the macrocycle plane of the porphyrin is ~10°. This is in good agreement with the experimental evaluation of the relative molecular orientation of C<sub>70</sub> and porphyrin. The charge transfer and the relative orientation between the two molecules is depicted in Figure 8, which shows the planar integrals of the charge difference between the combined system and the two isolated molecules. The net charge transfer

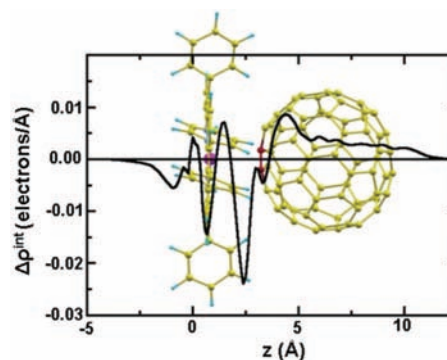


**Figure 8.** Planar integral of the difference in charge density between the combined system and the two isolated molecules. The relative position of the ZnTPP and C<sub>70</sub> in the complex is also shown.

toward the fullerene is clearly visible. In our calculations, the amount of this charge transfer is 0.05e, less than the 0.13e found in the calculations in ref 19.

We attribute this deviation to the different basis sets used in the calculations (localized basis set vs plane-wave basis). In any case, both calculations show that in the ground state the amount of charge transfer is quite small and the charge reorganization seems to go from the porphyrin to C<sub>70</sub>.

Figure 9 shows the highest occupied molecular orbital (HOMO), the HOMO-1, the lowest unoccupied molecular orbital (LUMO), and LUMO+1 of the porphyrin+C<sub>70</sub> system, similarly to what have been obtained by Basiuk et al. in the case of porphyrin–C<sub>60</sub> complexes.<sup>31</sup> It is worth noting that, although there is no molecular linker and the molecules are very close together, the HOMO orbitals are on the porphyrin molecule while the LUMO orbitals are on the C<sub>70</sub> molecule, and the same is true for the HOMO–1 and LUMO+1, respectively. Therefore, the HOMO and LUMO orbitals are “separated” on the two molecular species, so the excited-state interactions may be present in the contiguous chromophores and this system acts as a *donor/acceptor* junction.

## Discussion

The C1s core level spectra (XPS and NEXAFS) show that the majority of the features can be described with a superposition of the two pristine spectra (ZnTPP and C<sub>70</sub>), indicating that the electronic states (in the case of NEXAFS, the joint density of states) are the same as those for the separated molecules. Similar information is obtained from the ultraviolet photoemission spectroscopy (UPS) in the valence band region (see the Supporting Information), where the pristine valence band spectra can reproduce quite well the codeposited spectrum just with a shift of the ZnTPP spectrum toward the Fermi level and of the C<sub>70</sub> spectrum in the opposite direction. At the same time, the N1s core level spectra of the codeposited system are practically the same as those for the ZnTPP, if we exclude the shifts. XPS, NEXAFS, and UPS, therefore, indicate that the ground-state electronic spectra of the codeposited system reflect a simple summation of the pristine components, apart from small shifts due to the equalization of the Fermi level and the charge reorganization at the interface between ZnTPP and C<sub>70</sub>. Moreover, the line shape of the Zn3p states (data not shown) is similar to the spectrum of pure ZnTPP, indicating that the Zn remains in the center of the macrocycle and that the macrocycle is not bent or distorted because of the interaction with C<sub>70</sub>. These observations indicate also that the whole geometrical structure of the two single molecular species is conserved when the complex is formed.

(28) Giannozzi, P., et al. <http://www.quantum-espresso.org>.

(29) Perdew, J. P.; Burke, K.; Ernzerhof, M. *Phys. Rev. Lett.* **1996**, *77*, 3865.

(30) Vanderbilt, D. *Phys. Rev. B* **1990**, *41*, 7892.

(31) Basiuk, V. *J. Phys. Chem. A* **2005**, *109*, 3704.

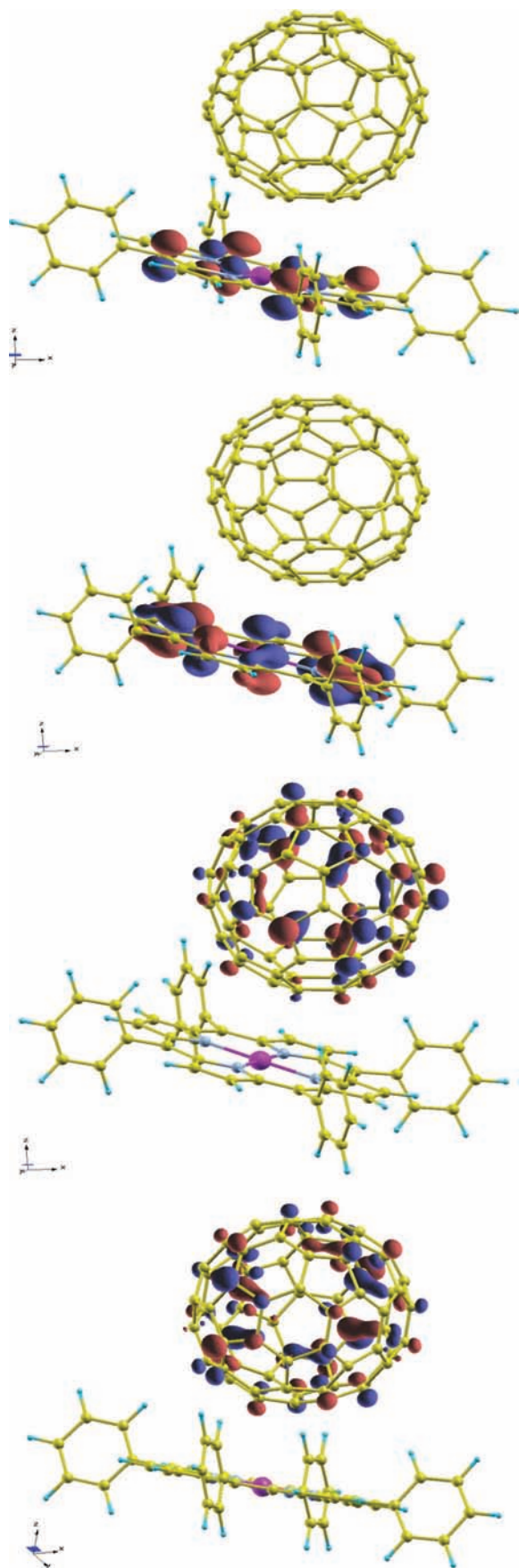


**Figure 9.** Kohn–Sham molecular orbitals of the porphyrin+C<sub>70</sub> system. From top to bottom the displayed orbitals are HOMO–1, HOMO, LUMO, and LUMO+1.

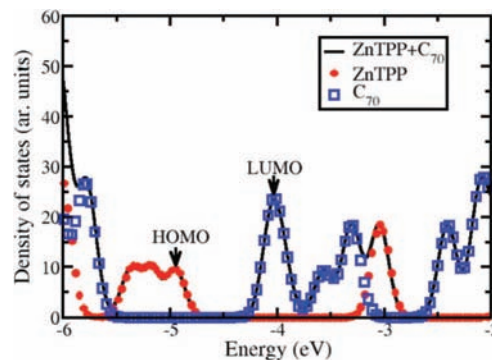


**Figure 10.** Computed density of states of the porphyrin (red), C<sub>70</sub> (blue), and porphyrin+C<sub>70</sub> (black) systems.

These experimental data were confirmed by our calculations in the ground state that show an amount of charge transfer that is quite small (the charge reorganization seems to go from the porphyrin to C<sub>70</sub>) and the pristine molecular structure is unchanged. In particular, Figure 10 shows the empty and filled density of states (DOS) of the porphyrin, C<sub>70</sub>, and porphyrin+C<sub>70</sub>. Even in the region where there are both C<sub>70</sub> and porphyrin states, and therefore an hybridization might occur, the DOS of the complex system is practically the superposition of the two DOS of the pristine molecules, indicating that in the electronic spectra of this material the pristine molecular ground-state perturbation is weak as obtained in our experimental data.

This situation changes when the excited-state interaction dynamics are considered. The ResPES data indicate the electrons excited into the first macrocycle empty state suddenly transfer to the C<sub>70</sub> on a time scale faster than 1–2 fs. Experimental data and calculations both suggest this system should act as a *donor/acceptor* junction. Upon photoexcitation an ultrafast electron transfer between donor and the proximate acceptor takes place, which ensures an efficient charge production that is the first step for the generation of photovoltaic current. Photovoltaic applications, however, need the separated charges to be collected at the electrodes, which is a considerably less efficient process, related to the unsolved problems of nanoscale morphology and vertical phase segregation of the dyad. This set of information is based on conformational and supramolecular design of the organic molecules; thus it is of fundamental interest to determine the adsorption geometry and the internal conformation of the donor–acceptor dyes.

In the present case C<sub>70</sub> brings the porphyrins into a tilted plane register, with an average angle of the macrocycle of 47°, as compared with the in-plane relationship observed in the porphyrin multilayer.<sup>13</sup> Although we have not measured the transport properties, the molecular arrangement found and the local geometrical correlation of the donor–acceptor system (“side-on” orientation of the C<sub>70</sub> molecule with respect to the macrocycle) are expected to favor the collection of the separated charges at the electrodes.

## Conclusions

The attraction of a fullerene to a porphyrin represents a supramolecular recognition element that allows the engineering of supramolecular solids on a mesoscopic scale. In fact, we were able to grow in an ultrahigh vacuum a self-assembled molecular complex composed by ZnTPP and C<sub>70</sub> codeposited on a semiconductor surface, where the two molecules assume a preferential reciprocal orientation in agreement with theoretical



models. We anticipate, also with our former work,<sup>14</sup> the present molecular design principles will be most useful in the manipulation of photophysical properties, in adjusting the charge transfer and in the creation of new (partly ordered) frameworks. In the present case, the ground-state electronic spectra of our codeposited material reflect a simple summation of components, so the ground-state perturbation is weak. However, the excited-state interactions are present in the contiguous chromophores, and this system acts as a *donor/acceptor* junction where the excited charges at the porphyrin macrocycle can rapidly delocalize to the fullerene. The time scale of the ultrafast charge transfer is smaller than 1–2 fs.

Finally, we observed that C<sub>70</sub> brings the porphyrins into a tilted plane register with the macrocycle at an average angle of ~47° from the substrate surface, which in organic photovoltaic

cells should probably increase the possibility to collect the separated charges at the electrodes.

**Acknowledgment.** This work is supported by the Italian Ministry of University and Research through PRIN-2006 020543 and PRIN-2006 022847.

**Supporting Information Available:** The valence band spectra measured at  $h\nu = 90$  eV of the codeposited system, of ZnTPP and C<sub>70</sub> multilayer and the sum of these two pristine spectra, the theoretically calculated N1s NEXAFS for ZnTPP-C<sub>70</sub> complex and the corresponding states that mainly contribute to the NEXAFS spectrum, information on the C1s NEXAFS spectrum as well as the Auger spectrum measured at  $h\nu = 389.07$  eV. This material is available free of charge via the Internet at <http://pubs.acs.org>.

JA806914G